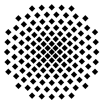

Universität Stuttgart

SimTech
Cluster of Excellence

A. Lauser[a] · **C. Hager**[b] · **R. Helmig**[a] · **B. Wohlmuth**[c]

A new approach for phase transitions in miscible multi-phase flow in porous media

Stuttgart, June 2010

[a] Institute of Hydraulic Engineering (IWS), University of Stuttgart,
Pfaffenwaldring 61, 70569 Stuttgart/ Germany
{lauser,helmig}@iws.uni-stuttgart.de

[b] Institute of Applied Analysis and Numerical Simulation (IANS), University of Stuttgart,
Pfaffenwaldring 57, 70569 Stuttgart/ Germany
hager@ians.uni-stuttgart.de

[c] M2 - Zentrum Mathematik, Technische Universität München,
Boltzmannstraße 3, 85748 Garching/ Germany
barbara.wohlmuth@ma.tum.de

Abstract Numerical simulation of non-isothermal multi-phase flow and transport processes in porous media is a very challenging task; Even more so, if miscibility effects cannot be neglected. One of the main reasons why miscibility tends to be problematic, is the need to incorporate phase transitions: On one hand, phase transitions are essential for the flow behaviour, on the other hand convergence of the nonlinear solver is severely impaired or even non-existent if they are not handled robustly.

In this work, we present a new and mathematically sound way of including these phase transitions into the nonlinear system of equations. First, they are formulated as a set of local inequality constraints; Thereafter, these are integrated directly into the nonlinear solver using a nonlinear complementarity function. By this, we can achieve local superlinear convergence of Newton's method. The improved robustness of the scheme is illustrated by several complex numerical examples.

Keywords Phase transition · Phase state · Multi-phase flow · Semismooth Newton · Porous media

Preprint Series **Issue No. 2010-34**
Stuttgart Research Centre for Simulation Technology (SRC SimTech)
SimTech – Cluster of Excellence
Pfaffenwaldring 7a
70569 Stuttgart
info@simtech.uni-stuttgart.de
www.simtech.uni-stuttgart.de

1 Introduction

Many practically relevant multi-phase problems for flow and transport in porous media require knowledge of the composition of the involved fluid phases in order to adequately approximate the underlying physical processes. Among others, these applications include CO_2 sequestration and storage [19], gas diffusion layers of polymer membrane fuel cells [1], and in-situ ground remediation [31]. One major issue of contemporary multi-phase multi-component models are phase transitions. A sound incorporation of these transitions into the flow model is essential since the appearance or disappearance of a fluid phase changes the underlying physics of the local problem. If not handeled properly, this tends to cause numerical oscillations when solving the nonlinear system of equations. Previous approaches like presented in [5, 8] locally adapt the choice of the primary variables to the phase state. Although this approach is applicable to some multi-phase, multi-component problems, it often leads to irregular convergence behaviour if the phase states are quickly changing, and to a drastic reduction of the time step size. Hence, there is a strong demand for a robust implicit numerical scheme for handling phase transitions, which is the goal of the present paper. For approaches involving explicit time integration and flash calculations, we refer to [9].

As shown in [5], a phase (dis)appears if some physical quantity excesses a given threshold. Based on this, we formulate the conditions for the local composition of the phases in a specific way, namely as a set of so-called complementarity or Karush–Kuhn–Tucker (KKT) conditions, leading to the mathematical structure of a variational inequality [7, 11, 23]. As similar conditions also occur in other important applications like contact or obstacle problems [22], there exist many different approaches to treat these nonlinear complimentarity constraints; we refer to [10] for an overview of most of the methods. In this paper, we make use of the fact that the KKT conditions can equivalently be reformulated as a non-differentiable but semismooth equation, termed nonlinear complementarity (NCP) function [2, 7, 14, 26]. Combined with the balance equations, a system of nonlinear equations is obtained that can be solved by means of a semismooth Newton method with locally superlinear convergence [7, 29]. As the KKT conditions and the nonlinearities of the material are handeled within the same Newton loop, a nested iteration for the determination of the local phase state is avoided. Due to the local character of the phase conditions, the Newton method can efficiently be implemented in terms of an active set strategy [14, 15, 20]. The generality and robustness of this approach has been shown in, e.g., [12, 21, 24, 28].

The rest of this work is structured as follows: In Section 2, we specify the general physical conservation equations as well as the KKT conditions describing the phase transitions. In Section 3, we sketch the discretization method, show that the local inequality constraints can be reformulated as a semismooth equation, and outline how the resulting problem can be solved by a semismooth Newton method. Section 4 contains the numerical results; after specifying some technicalities of the implementation in Section 4.1, the physical correctness of our new approach is verified by means of a benchmark example. In Subsection 4.3, the model is compared with the primary variable switching approach proposed in [5], followed by a three-dimensional example simulating the sequestration of carbon dioxide. Finally, we conclude in Section 5.

2 Governing equations

We consider a Mp-Nc system with N different components ($\cdot^1$ to $\cdot^N$) as well as with M different phases, ordered by their wettability with $\cdot_1$ being the least wetting one (gas phase). Assuming that the fugacity of any component K is the same in all phases, we have a priori the following $MN+2M+N+1$ unknowns summarized in Table 1.

T	temperature
p_α	pressure in phase $\alpha \in \{1, \dots, M\}$
S_α	saturation of phase $\alpha \in \{1, \dots, M\}$
f^K	fugacity of comp. $K \in \{1, \dots, N\}$
x_α^K	mole fraction of comp. $K \in \{1, \dots, N\}$ in phase $\alpha \in \{1, \dots, M\}$

Table 1: List of physical unknowns

In the following, we derive several relations for the above unknowns, originating from the physical balance laws and constitutive equations based on local thermodynamic equilibrium.

2.1 Balance equations

ϕ	porosity
q^K	mass source term of component K
q^h	heat source term
$\mathbf{K}$	permeability tensor
$\mathbf{g}$	gravity acceleration vector
M^K	molar mass of component K
ρ_s	density of the solid phase
c_s	specific heat capacity of the solid phase
$\mu_\alpha(T)$	viscosity of phase α
$\rho_{\mathrm{mol},\alpha}(p_\alpha, x_\alpha^K, T)$	molar density of phase α
$\rho_{\mathrm{mass},\alpha}(p_\alpha, x_\alpha^K, T)$	mass density of phase α
$u_\alpha(p_\alpha, x_\alpha^K, T)$	specific internal energy of phase α
$h_\alpha(p_\alpha, x_\alpha^K, T)$	specific enthalpy of phase α
$k_{r\alpha}(S_\alpha)$	relative permeability of phase α
$\lambda_{\mathrm{pm}}(p_\alpha, x_\alpha^K, S_\alpha, T)$	heat conduction coefficient

Table 2: List of physical parameters. The dependence on the unknowns stated in Table 1 is indicated.

We assume that the multiphase Darcy law is valid as the equation for conservation of momentum; thus, we obtain $N+1$ partial differential equations describing the balance of component masses and energy. Each balance equation has the form

$$\frac{\partial \xi}{\partial t} - \nabla \cdot \Psi - q = 0, \tag{1}$$

with a storage term ξ, a flux term Ψ and a source term q. Assuming that diffusive mass fluxes can be neglected in all phases [5], conservation of mass for component $K \in \{1, \dots, N\}$ is given by (1) with

$$\begin{aligned} \xi &= \phi \sum_{\alpha=1}^{M} \rho_{\mathrm{mol},\alpha} x_\alpha^K S_\alpha, \\ \Psi &= \sum_{\alpha=1}^{M} \left(\frac{k_{r\alpha}}{\mu_\alpha} \rho_{\mathrm{mol},\alpha} x_\alpha^K \mathbf{K} \left(\nabla p_\alpha - \rho_{\mathrm{mass},\alpha} \mathbf{g} \right) \right), \quad q = q^K, \end{aligned} \tag{2}$$

with the supplementary equation

$$\rho_{\mathrm{mass},\alpha} = \rho_{\mathrm{mol},\alpha} \sum_{K=1}^{N} x_\alpha^K M^K.$$

The conservation of energy yields relation (1) with

$$\begin{aligned} \xi &= \phi \sum_{\alpha=1}^{M} \rho_{\mathrm{mass},\alpha} u_\alpha S_\alpha + (1-\phi) \rho_s c_s T, \\ \Psi &= \sum_{\alpha=1}^{M} \left(\frac{k_{r\alpha}}{\mu_\alpha} \rho_{\mathrm{mass},\alpha} h_\alpha \mathbf{K} \left(\nabla p_\alpha - \rho_{\mathrm{mass},\alpha} \mathbf{g} \right) \right) + \lambda_{\mathrm{pm}} \nabla T, \quad q = q^h. \end{aligned} \tag{3}$$

In (2) and (3), we have used the parameters stated in Table 2.

2.2 Constitutive relations

Next, we look at the constitutive relations between the quantities given in Table 1, for which we assume the system to be in local thermodynamic equilibrium. Starting with the sum of the saturations, we get

$$\sum_{\alpha=1}^{M} S_\alpha = 1. \tag{4}$$

For the phase pressures p_α, we obtain the following $(M-1)$ equations, due to the assumed order of the wettabilities:

$$p_{\alpha-1} - p_\alpha = p_{c,(\alpha-1)\alpha}, \quad \alpha \in \{2, \dots, M\}, \tag{5}$$

with the capillary pressure $p_{c,(\alpha-1)\alpha} = p_{c,(\alpha-1)\alpha}(S_\alpha)$ depending on the saturation S_α of the phase with higher wettability [27]. For the modeling of the capillary pressure, the approaches of Brooks and Corey or van Genuchten are commonly used, depending on the structure of the porous medium [13].

Next, we discuss the relations between the fugacities f^K, $K \in \{1, \dots, N\}$, and the mole fractions x_α^K, $K \in \{1, \dots, N\}$, $\alpha \in \{1, \dots, M\}$. For this, we need to distinguish between the gas and the liquid phases. For the gas phase, the fugacity f^K can be determined from the corresponding mole fractions, the total gas pressure p_1 and the fugacity coefficient $\Phi^K = \Phi^K(p_1, x_1^1, \dots, x_1^N, T)$:

$$f^K = \Phi^K x_1^K p_1, \quad K \in \{1, \dots, N\}. \tag{6}$$

In the common special case that the gas phase can be considered as an ideal gas, we have $\Phi^K = 1$, and (6) simplifies to $f^K = x_1^K p_1$ for any component K.

For the liquid phases, we make use of the activity coefficients $\gamma_\alpha^K = \gamma_\alpha^K\left(p_\alpha, x_\alpha^1, \dots, x_\alpha^N, T\right)$, $\alpha \in \{2, \dots, M\}$, to obtain the relations

$$f^K = \gamma_\alpha^K x_\alpha^K, \quad K \in \{1, \dots, N\}, \quad \alpha \in \{2, \dots, M\}. \tag{7}$$

Using (5), (6) and supposing that the gas pressure p_1, the composition of the gas phase and the temperature T are known, (7) can be interpreted as a nonlinear system for the mole fractions $\{x_\alpha^K\}_{K\in\{1,\dots,N\}}$. In the following, we assume that this system can uniquely be solved for the latter quantities, leading to some nonlinear relations

$$x_\alpha^K = g_\alpha^K\left(p_1, x_1^1, \dots, x_1^N, T\right), \quad K \in \{1, \dots, N\}, \quad \alpha \in \{2, \dots, M\}. \tag{8}$$

As in the case of the fugacity coefficients Φ^K a common special case exists: If the miscibility of the components is very low, the function g_α^K in (8) can easily be determined by combining the relations of Henry and Raoult, as outlined for the case $M = N = 2$ in Example 1 below.

Example 1 We consider a two-phase, two-component system with nonwetting $(\cdot_1)$ and wetting phase $(\cdot_2)$. Further, we suppose that component $\cdot^1$ is air and $\cdot^2$ is water. Assuming the gas phase behaves as an ideal gas, we can compute the fugacities from (6):

$$f^1 = x_1^1 p_1, \quad f^2 = x_1^2 p_1.$$

We remark that in this case, the fugacities correspond to the partial pressures of the components in the gas phase.

Further, supposing that the mole fraction x_2^2 of water in the wetting phase is close to one, Raoult's law gives the relation

$$f^2 = p_{\text{vap}}^2 x_2^2 \quad \rightarrow \quad x_2^2 = \frac{f^2}{p_{\text{vap}}^2} = \frac{p_1}{p_{\text{vap}}^2} x_1^2, \tag{9}$$

with $p_{\text{vap}}^2 = p_{\text{vap}}^2(T)$ denoting the vapor pressure of water.

The remaining mole fraction x_2^1 of air in the wetting phase can be determined from (7) and Henry's law with the Henry coefficient $H_2^1 = H_2^1(T)$:

$$f^1 = H_2^1 x_2^1 \quad \rightarrow \quad x_2^1 = \frac{f^1}{H_2^1} = \frac{p_1}{H_2^1} x_1^1. \tag{10}$$

Remark 1 We assume that the relations (6) and (8) hold even if one of the phases involved, e.g., phase α, is not present at the given spatial point. In this case, there is no physical interpretation of the molar fractions x_α^K, $K \in \{1, \dots, N\}$. Hence, these values can in principal be chosen arbitrarily which we do by means of (6), (8). The conditions for the presence of phase α are described in the next subsection.

2.3 Phase transitions

So far, we have obtained $MN + M + N + 1$ equations for the $MN + 2M + N + 1$ unknowns stated in Table 1. The missing M relations are derived from the number of phases present at a given spatial point. For each phase $\alpha \in \{1, \dots, M\}$, we observe that the sum of the corresponding mole fractions is bounded from above by one, with equality holding if the phase is present:

$$\sum_{K=1}^{N} x_\alpha^K \leq 1, \qquad \sum_{K=1}^{N} x_\alpha^K = 1 \text{ if phase } \alpha \text{ is present.} \tag{11}$$

Combining (11) with the nonnegativity of the saturation S_α, we obtain the following complementarity conditions:

$$1 - \sum_{K=1}^{N} x_\alpha^K \geq 0, \qquad S_\alpha \geq 0, \qquad S_\alpha \left(1 - \sum_{K=1}^{N} x_\alpha^K\right) = 0, \quad \alpha \in \{1, \dots, M\}. \tag{12}$$

The last equation in (12) expresses the fact that a strict inequality in (11) can only hold if the phase is not present, i.e., if the saturation is zero.

2.4 Choice of primary variables

For the solution of the coupled system (1), (12), most of the $MN+2M+N+1$ unknowns are eliminated by means of the constitutive laws stated in Section 2.2. For this, we reformulate (4) and (5) to

$$S_1 = 1 - \sum_{\alpha=2}^{M} S_\alpha, \qquad p_\alpha = p_1 - \sum_{\beta=2}^{\alpha} p_{c,(\beta-1)\beta}(S_\beta), \quad \alpha \in \{2, \dots, M\}. \tag{13}$$

Substituting the relations (6), (8), (13) into the system (1), (12), we can reduce the number of unknowns to $N + M + 1$, which we choose as

$$\kappa := \Big(p_1, x_1^1, \dots, x_1^N, S_2, \dots, S_M, T\Big), \tag{14}$$

In other words, our primary variables are the pressure of the gas phase, its mole fractions with respect to the N components, $M - 1$ saturations and the temperature.

Remark 2 In [5], the phase transition constraints are also considered as constitutive relations, leading to a system with only $N+1$ primary variables whose choice depends on the composition of the phases. To illustrate this approach, we consider the 2p-2c system of Example 1. If for example only the wetting phase is present at a given spatial point, we have $x_2^1 + x_2^2 = 1$ from (11) and $S_2 = 1$ from (4). Hence, taking the unknown x_1^1 as primary variable, the remaining mole fraction x_1^2 can be calculated from (9), (10) and (11). In contrast, if both phases are present, all mole fractions can be computed from (11) and the saturation S_2 becomes the primary variable.

Our approach is different, as we have a larger but fixed set of primary variables and include the KKT conditions (11) into the system to be solved at each time step. Because of $N + M + 1 > N + 1$, this a priori leads to a larger system matrix. However, due to the local nature of (11), we can easily reduce the size of the tangent system to $N + 1$ by static condensation. Details are given in Section 3.3.

Remark 3 The choice (14) is not unique. Instead of the mole fractions x_1^K, one can for example use the fugacities f^K or, if only a two-phase system is considered, the mole fractions x_2^K of the wetting phase. For the numerical results in Section 4 dealing with a 2p-2c system, we have used the latter possibility, i.e., the primary variables are chosen as

$$\kappa_{\text{alg}} := \Big(p_1, x_2^1, x_2^2, S_2, T\Big). \tag{15}$$

The resulting coupled system that needs to be solved for (14) contains the nonlinear partial differential equations (1) as well as the inequality constraints in (12); hence, it cannot be solved analytically. In the following section, we describe how the exact solution of this complex problem is approximated numerically.

3 Discretization and numerical algorithm

3.1 Discretization

Equations (1) are discretized on an unstructured conforming mesh T_h with mesh size h consisting of triangles and quadrilaterals in the case of two spatial dimensions or tetrahedra, pyramids, prisms and hexahedra for three dimensions. For T_h we chose the space of the lowest order conforming finite element functions V_h and the space of test functions W_h for which we select the characteristic functions of vertex centered finite volumes [13]. Using the implicit Euler discretization in time and the abbreviation $(u, v)_\Omega = \int_\Omega uv \,\mathrm{d}x$, we get the discrete form

$$\frac{1}{t^{k+1} - t^k} \left[\left(\xi^{k+1}, w_h\right)_\Omega - \left(\xi^k, w_h\right)_\Omega\right] - \left(\nabla \cdot \Psi^{k+1}, w_h\right)_\Omega - \left(q^{k+1}, w_h\right)_\Omega = 0 \tag{16}$$

for all test functions $w_h \in W_h$. The superscripts $\cdot^k$ and $\cdot^{k+1}$ are associated with the time levels t^k and t^{k+1}. After inserting a basis function representation

$$\kappa = \sum_{j \in \mathcal{N}} \hat{\kappa}_j N_j \tag{17}$$

of the unknown finite element functions for the $N + M + 1$ primary variables κ given in section 2.4 (where N_j denotes the j-th finite element ansatz function, $\mathcal{N}$ is the set of nodes in the mesh T_h, and $\hat{\kappa}_j \in \mathbb{R}^{N+M+1}$) and evaluating the integrals, we obtain a system of nonlinear algebraic equations for the coefficients $\hat{\kappa}_j$:

$$\mathbf{F}(\kappa) = \mathbf{0}. \tag{18}$$

Here, the vector $\kappa = \kappa^{k+1} \in \mathbb{R}^{(N+M+1)\,|\mathcal{N}|}$ contains all unknowns at time t^{k+1}, but in the following we omit the time index $\cdot^{k+1}$ for ease of notation. The time levels t^k and t^{k+1} as well as the last known solution κ^k are known parameters of the nonlinear function $\mathbf{F} : \mathbb{R}^{(N+M+1)\,|\mathcal{N}|} \to \mathbb{R}^{(N+1)\,|\mathcal{N}|}$.

3.2 Semi-smooth equality conditions

As we have $N + M + 1 > N + 1$, the nonlinear system (18) needs to be completed with the nodal version of the complementarity conditions (12) given by

$$1 - \sum_{K=1}^{N} (x_\alpha^K)_j \geq 0, \qquad (S_\alpha)_j \geq 0, \qquad (S_\alpha)_j \left(1 - \sum_{K=1}^{N} (x_\alpha^K)_j\right) = 0, \tag{19}$$

for every $\alpha \in \{1, \ldots, M\}$, $j \in \mathcal{N}$. In order to treat (18) and (19) within the same Newton iteration, we rewrite the latter constraints as an equality by means of the following equation:

$$(S_\alpha)_j - \max\left\{0, (S_\alpha)_j - c_\alpha \left(1 - \sum_{K=1}^{N} (x_\alpha^K)_j\right)\right\} = 0. \tag{20}$$

with a fixed constant $c_\alpha > 0$. With this, we obtain the following lemma:

Lemma 1 *The inequality constraints* (19) *are equivalent to the equality* (20) *for any constant* $c_\alpha > 0$.

Proof First, we show that (20) implies (19), omitting the lower indices j, α for ease of notation. Let $c > 0$ be a fixed constant. We distinguish between two different cases, according to the value of the max-function in (20):

(*i*) $S - c\left(1 - \sum_{K=1}^{N} x^K\right) \leq 0$:
In this case, (20) simplifies to $S = 0$, implying that $c\left(1 - \sum_{K=1}^{N} x^K\right) \geq 0$ holds. With $c > 0$, the complementarity conditions (19) follow.

(*ii*) $S - c\left(1 - \sum_{K=1}^{N} x^K\right) > 0$:
In this case, (20) becomes $c\left(1 - \sum_{K=1}^{N} x^K\right) = 0$, such that $S > 0$ is necessarily fulfilled. Again, the inequality constraints (19) are satisfied.

The implication (19) $\Rightarrow$ (20) can be shown similarly and is omitted here.

Remark 4 There are other possibilities than (20) to define a nonlinear complementarity function that is equivalent to (19) (see, e.g., [7] and the references therein). The reason for using Equation (20) is its piecewise linearity with respect to the variables S_α, x_α^K.

The proof of Lemma 1 directly implies that the degrees of freedom of the solution of (19) can be partitioned into the following (in)active sets:

$$\mathcal{A}_\alpha := \left\{ j \in \mathcal{N} : (S_\alpha)_j - c_\alpha \left(1 - \sum_{K=1}^{N} (x_\alpha^K)_j\right) > 0 \right\}, \qquad \mathcal{I}_\alpha := \mathcal{N} \backslash \mathcal{A}_\alpha. \tag{21}$$

In combination with (20), the degrees of freedom in the active set $\mathcal{A}_\alpha$, $\alpha \in \{1, \ldots, M\}$, correspond to those nodes where the phase α is present.

Using (8) and (13), we can rewrite the phase change constraints (20) in terms of the primary variable vector κ given in (18), yielding the system of nondifferentiable equations

$$\mathbf{C}(\kappa) := (C_\alpha(\kappa_j))_{j \in \mathcal{N}}^{\alpha \in \{1,\ldots,M\}} = \mathbf{0} \tag{22}$$

with

$$C_1(\kappa_j) := 1 - \sum_{\alpha=2}^{M} (S_\alpha)_j - \max\left\{0, 1 - \sum_{\alpha=2}^{M} (S_\alpha)_j - c_1 \left(1 - \sum_{K=1}^{N} \left(x_1^K\right)_j\right)\right\}, \tag{23a}$$

$$C_\alpha(\kappa_j) := (S_\alpha)_j - \max\left\{0, (S_\alpha)_j - c_\alpha \left(1 - \sum_{K=1}^{N} g_\alpha^K(\kappa_j)\right)\right\}, \alpha \in \{2, \ldots, M\}. \tag{23b}$$

3.3 Newton scheme

The complementarity functions (23) are piecewise differentiable and thus in particular semismooth [7], such that a generalized variant of the Newton scheme for semismooth problems can be used to solve the system (18), (23). The procedure is basically the same as the standard Newton method in all regions where the functions are differentiable; at the other points, the values of the partial derivatives are defined by extending one of the derivatives from the neighborhood of this point. For the exact definition of semismoothness, we refer to [4, 7, 14], a detailed overview of Newton methods for nonlinear problems is given in [6].

If $\kappa^{(l)}$ stands for the values of the primary variables after the l-th Newton iteration, a linear system has to be solved for the Newton update $\Delta\kappa^{(l)}$, leading to the next iterate $\kappa^{(l+1)} = \kappa^{(l)} + \Delta\kappa^{(l)}$. The partial derivatives of the smooth but highly nonlinear function (18) can be computed approximately using central differences. This is not feasible for the NCP functions (23) which are only piecewise

smooth; however, due to their rather easy structure, the partial derivatives can be calculated explicitly. At the l-th Newton iteration, the values of (23) depend on the following approximate active sets

$$\mathcal{A}_1^{(l)} := \left\{ j \in \mathcal{N} : 1 - \sum_{\alpha=2}^{M} (S_\alpha)_j^{(l)} - c_\alpha \left(1 - \sum_{K=1}^{N} \left(x_1^K \right)_j^{(l)} \right) > 0 \right\}, \tag{24a}$$

$$\mathcal{A}_\alpha^{(l)} := \left\{ j \in \mathcal{N} : (S_\alpha)_j^{(l)} - c_\alpha \left(1 - \sum_{K=1}^{N} g_\alpha^K \left(\kappa_j^{(l)} \right) \right) > 0 \right\}, \tag{24b}$$

and the corresponding inactive sets $\mathcal{I}_\alpha^{(l)} := \mathcal{N} \backslash \mathcal{A}_\alpha^{(l)}$, $\alpha \in \{1, \dots, M\}$. These sets may change several times during the Newton loop, but if the Newton method converges, the final active sets are the same as those defined in (21).

Remark 5 The consistent treatment of the phase transitions within the Newton loop has the advantage that no outer fixed point iteration for the determination of the physically correct phase state is necessary. This saves a substantial amount of computation time. Furthermore, the Newton iteration is rather robust with respect to the initialization of the active sets (24), such that larger time steps can be used. Some numerical examples are presented in Section 4.

Using (24), we can easily compute the Newton equation of (23):

$$C_1(\kappa_j^{(l)}): \quad \begin{cases} \sum_{\alpha=2}^{M} (\Delta S_\alpha)_j^{(l)} = 1 - \sum_{\alpha=2}^{M} (S_\alpha)_j^{(l)}, & j \in \mathcal{I}_1^{(l)}, \\ \sum_{K=1}^{N} (\Delta x_1^K)_j^{(l)} = 1 - \sum_{K=1}^{N} (x_1^K)_j^{(l)}, & j \in \mathcal{A}_1^{(l)}, \end{cases} \tag{25a}$$

$$C_\alpha(\kappa_j^{(l)}): \quad \begin{cases} (\Delta S_\alpha)_j^{(l)} = -(S_\alpha)_j^{(l)}, & j \in \mathcal{I}_\alpha^{(l)}, \\ \sum_{K,L=1}^{N} \frac{\partial g_\alpha^K}{\partial x_1^L}(\kappa_j^{(l)})(\Delta x_1^L)_j^{(l)} = 1 - \sum_{K=1}^{N} (\Delta g_\alpha^K)_j^{(l)}, & j \in \mathcal{A}_\alpha^{(l)}, \end{cases} \tag{25b}$$

with the abbreviation

$$(\Delta g_\alpha^K)_j^{(l)} := g_\alpha^K(\kappa_j^{(l)}) + \frac{\partial g_\alpha^K}{\partial p_1}(\kappa_j^{(l)})(\Delta p_1)_j^{(l)} + \frac{\partial g_\alpha^K}{\partial T}(\kappa_j^{(l)})(\Delta T)_j^{(l)}.$$

From (25), one can see that the value of the constants c_α does not influence the equations of the Newton iteration. Furthermore, the special form of (25) can be used for a local static condensation, reducing the total size of the tangential system to $(N+1)|\mathcal{N}| \times (N+1)|\mathcal{N}|$ which is the same size as for the method presented in [5]. The condensation procedure is illustrated by means of the following example for $N = M = 2$, with the same notation as in Example 1.

Example 2 We consider a node $j \in \mathcal{N}$ with $j \in \mathcal{I}_1^{(l)} \cap \mathcal{A}_2^{(l)}$, i.e., only the wetting phase $\cdot_2$ is present at the l-th Newton iteration. For simplicity, we omit the upper index $\cdot^{(l)}$ and the lower index $\cdot_j$. From Example 1, we obtain that the functions g_2^K are only dependent on x_1^K, leading to

$$\sum_{K,L=1}^{2} \frac{\partial g_\alpha^K}{\partial x_1^L}(\kappa) \Delta x_1^L = \sum_{K=1}^{2} \frac{\partial g_\alpha^K}{\partial x_1^K}(\kappa) \Delta x_1^K = \frac{p_1}{H_2^1(T)} \Delta x_1^1 + \frac{p_1}{p_{\text{vap}}^2(T)} \Delta x_1^2.$$

For this case, the Newton equations (25) read

$$\Delta S_2 = 1 - S_2, \tag{26a}$$

$$\sum_{K=1}^{2} \frac{\partial g_\alpha^K}{\partial x_1^K}(\kappa) \Delta x_1^K = 1 - \sum_{K=1}^{2} \Delta g_\alpha^K. \tag{26b}$$

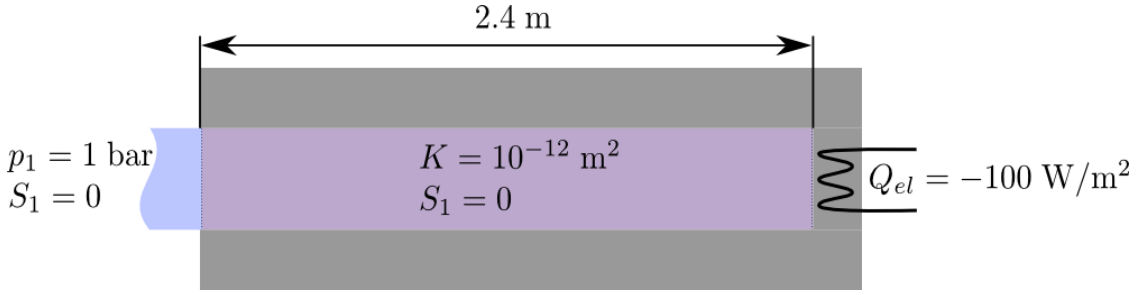

Fig. 1: The setup of the heat pipe problem used for physical validation.

For $p_1 > 0$, (26b) can for example be resolved for Δx_1^2:

$$\Delta x_1^2 = \frac{p_{\text{vap}}^2(T)}{p_1}\left(1 - \sum_{K=1}^{2} \Delta g_\alpha^K - \frac{p_1}{H_2^1(T)}\Delta x_1^1\right). \tag{27}$$

Substituting (26a), (27) into the global Jacobian matrix yields a system with only three local unknowns $(\Delta p_1, \Delta x_1^1, \Delta T)_j^{(l)}$ instead of the former five local variables. The remaining two unknowns $(\Delta S_2, \Delta x_1^2)_j^{(l)}$ can be computed afterwards in a local post-processing step using (26a), (27).

4 Numerical results

4.1 Implementation

The nonlinear system (18), (22) is solved using the Newton method described in section 3.3 with a variable time step size. In order to get an estimate of the robustness of the scheme, we use the following heuristic to determine the convergence radius of the Newton method: If the computation with a given time step size $t^{k+1} - t^k$ converges within at most 40 iterations, $t^{k+1} - t^k$ is increased by 25% while t^k is held constant and the Newton method is started anew with the solution of the previous time level (i.e. $\kappa^{k+1,(0)} \leftarrow \kappa^k$). This procedure is repeated until convergence cannot be achieved anymore, whereupon t^{k+1} is advanced by the result from the largest converged time step. This procedure allows to estimate the robustness of our method by comparing the obtained time step sizes with those obtained by using the primary variable switching model presented in [5].

As linear solver, a stabilized bi-conjugate gradient method is used in combination with an incomplete LU-decomposition as preconditioner [30]. To store the global Jacobian matrix, the compressed row storage layout is used [3] in conjunction with nested $(N + M + 1) \times (N + M + 1)$ matrices. It should be noted that – depending on the ratio of the largest and the smallest activity coefficients γ_α^K in any liquid phase $\alpha \in \{2, \dots, M\}$ – the blocks on the main diagonal of the tangential matrix may be quite ill-conditioned. For example, the rather typical water-air system outlined in Example 1, may exhibit ratios between the maximal entries of two different rows of a block in excess of 18 decimal orders of magnitude at $T = 25\,°\text{C}$ and $p_1 = 1\,\text{bar}$. But by using an incomplete LU decomposition as preconditioner, this does not pose a problem for convergence of the linear solver.

4.2 Physical validation

We verify the physical and numerical accuracy of our model by applying it to the heat pipe effect as described by Udell [32]. The setup of this problem with $M = 2$ phases and $N = 1$ component consists of an insulated pipe containing a porous medium which is initially fully saturated by liquid water and is depicted in Figure 1. At the left side of the pipe, a Dirichlet condition of 70 °C for temperature, liquid saturation of 100 % and liquid phase pressure of 1 bar is applied, while at the other end of the pipe, an electric heating element is modeled by a energy influx Neumann condition of $Q_{\text{el}} = -100\,\text{W/m}^2$. The steady-state solution for this problem can be obtained by observing that the mass flux of the liquid

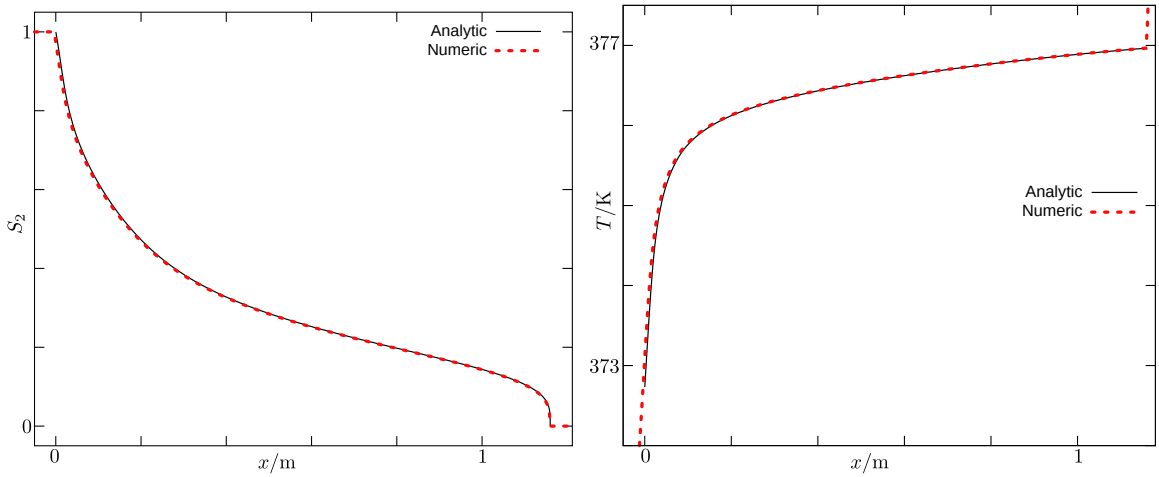

(a) Liquid saturation (b) Temperature

Fig. 2: Results for the semi-analytic and the numerical solutions of the heat pipe effect with respect to the position x. The origin of the x-axis is set to the position where the two-phase region starts.

phase is the reverse of the flux of the gas phase and that the sum of the energies transferred due to thermal conductivity of the porous medium and due to enthalpy transport of the fluids is equal to the power of the heating element. If gravity is neglected, this leads to the following system of ordinary differential equations which is valid for the two-phase region and can be solved using Runge-Kutta methods:

$$\frac{\partial p_1}{\partial S_2} = \frac{\frac{\partial p_c}{\partial S_2}}{1 + \frac{\nu_2}{\nu_1}\frac{k_{r1}}{k_{r2}}}, \qquad \frac{\partial x}{\partial S_2} = -\frac{\partial p_1}{\partial S_2}\frac{\lambda\left(\frac{\partial p_{\text{vap}}}{\partial T}\right)^{-1} + h_{\text{vap}}\frac{k_{r1}}{\nu_1}}{Q_{\text{el}}}$$

In this context,

$$\lambda = \lambda_{\text{dry}} + \sqrt{S_2}(\lambda_{\text{wet}} - \lambda_{\text{dry}})$$

stands for the heat conductivity of the medium at a given liquid saturation, p_{vap} represents the saturation pressure of water, ν_2 and ν_1 are the kinematic viscosities of the liquid and the gas phases and h_{vap} is the specific enthalpy of vaporization of water. For the fluid properties of water, the IAPWS industrial formulation is used [16, 18].

As capillary pressure relation, we use the Leverett function [25]

$$p_c = p_0\gamma\Big(1.263(1-S_2)^3 - 2.120(1-S_2)^2 + 1.417(1-S_2)\Big),$$

where $\gamma = 0.05878\text{Nm}^{-1}$ stands for the surface tension of water at 100.5°C, and $p_0 = \sqrt{\phi/K}$ is the scaling pressure. The latter assumes that the diameter of the meniscus of an average capillary is proportional to the porosity ϕ and reciprocal to the hydraulic conductivity K of the medium. The relative permeabilities are defined by

$$k_{r2} = S_2^3, \qquad k_{r1} = (1-S_2)^3$$

for the liquid and gas phase, respectively.

For the semi-analytic solution, the temperature is obtained by inverting the saturation pressure function, i.e. $T = p_{\text{vap}}^{-1}(p_1)$; For the numerical simulation, the domain size chosen is 2.4 m and is discretized using 200 uniform one-dimensional line segments. We remark that the size of the domain is irrelevant provided that it is large enough to contain the entire two-phase region.

The results obtained using our numerical model are in good agreement with the semi-analytic solution, as can be seen from Figure 2. Figure 2a shows the liquid phase saturation with respect to the distance from the position where the two-phase region starts, while 2b displays the temperature. These results demonstrate that the approximate solutions obtained from our model are physically meaningful.

4.3 Comparison to primary variable switching

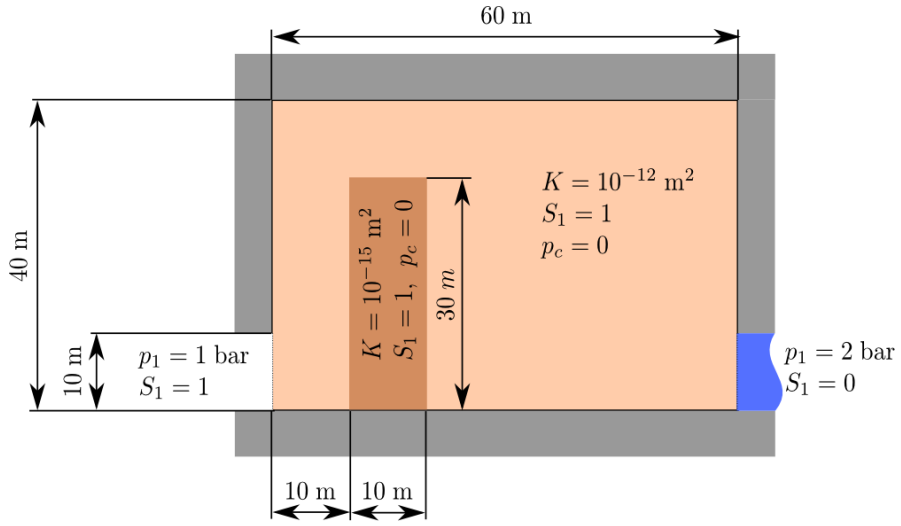

Fig. 3: The domain, initial and boundary conditions for the "obstacle" problem.

Next, we compare our model with the approach based on local switching of the primary variables as proposed by Class et al. [5]. For this purpose, we simulate the two-dimensional water injection problem outlined in Figure 3 with $M = N = 2$. The domain has a size of 60 m in the horizontal and 40 m in the vertical direction, with an acceleration of -9.81 m/s^2 in vertical direction due to gravity. The domain features a rectangular obstacle consisting of a medium with low permeability which is embedded into a material with higher permeability. The temperature is assumed to be constant at 25°C, and the whole domain is initially fully saturated by molecular nitrogen at $p_1 = 1$ bar. No-flow Neumann boundary conditions are chosen everywhere except for the lower left and the lower right boundaries. The lower right serves as an inlet of liquid water, with a pressure of $p_1 = 2$ bar and $S_2 = 100\%$, while the lower left is chosen as outlet with $p_1 = 1$ bar and $S_2 = 0\%$. We use the IAPWS industrial formulation [16, 18]

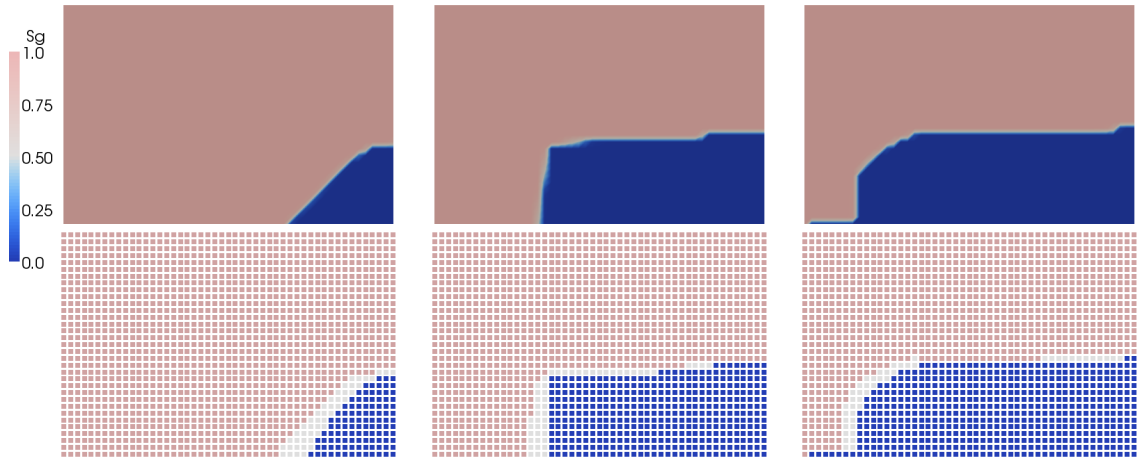

(a) $t = 6 \cdot 10^5$ s (b) $t = 5.5 \cdot 10^6$ s (c) Steady state

Fig. 4: The evolution of the saturation S_1 and of the active sets for the obstacle problem.

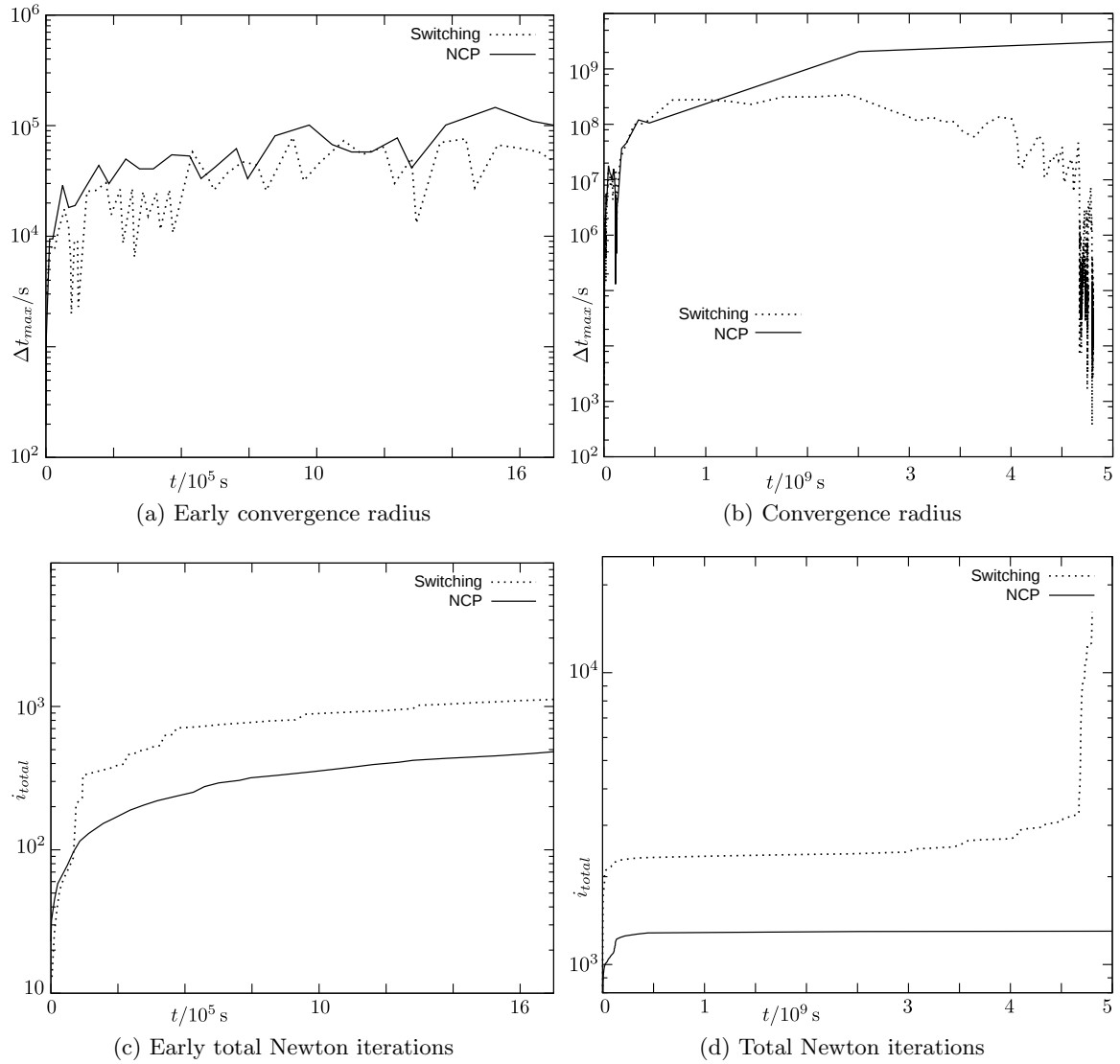

(a) Early convergence radius

(b) Convergence radius

(c) Early total Newton iterations

(d) Total Newton iterations

Fig. 5: Comparision of the performance of our model and the primary variable switching approach: (a) and (b) show the convergence radius of both models as determined by the procedure given in Section 4.1 with respect to the experiment time, (c) and (d) plot the total number of iterations needed to reach a certain experiment time if the time step size is always chosen to be the model's convergence radius.

for the properties of water, the Henry coefficients of nitrogen given by IAPWS in [17], and assume nitrogen as an ideal gas.

For this problem, the porosity is 40% all over the domain, the residual saturations as well as the capillary pressure are set to zero, and the relative permeability for phase α is assumed to be equal to the corresponding saturation, i.e., $k_{r\alpha} = S_\alpha$.

Figure 4 shows the evolution of the gas saturation as well as the distribution of the active sets computed with our new approach. We do not display the results for the primary variable switching model, as the differences of the solutions are negligible. First, the liquid water infiltrates quickly until it reaches the obstacle as can be seen in Figure 4a. Next, the saturation front climbs along the obstacle until it attains the hydrostatic pressure and begins to infiltrate into the obstacle, as outlined in Figure 4b. Finally, the system arrives at the steady state depicted in Figure 4c.

The two upper plots of Figure 5 show the convergence radius on a logarithmic scale for both models with respect to the simulation time. From the graphs, it can be concluded that both approaches

can be used for the early phase of the experiment where finding the correct phase state is not the limiting factor. However, shortly before steady state is reached, the primary variable switching approach experiences a serious breakdown which stems from oscillations in the phase state, while our new model does not exhibit this behavior. The two lower plots of Figure 5 show the total number of Newton iterations necessary to reach a specific time if the maximal time step size determined as in Section 4.1 is used. These two plots can be interpreted as proportional to the CPU time required for the simulation. Hence, one can observe that the new model allows for a substantial saving of computational time due to the increased robustness of the scheme.

In our experience, the method presented in this work typically exhibits a much more benign convergence behaviour than the primary variable switching approach, such that the benchmark presented here is a typical case rather than an exception.

4.4 Application: CO_2 sequestration and methane recovery

As a final example, we apply our scheme to a more complex three-dimensional problem simulating the injection of CO_2 into the soil and the subsequent extraction of methane at a different location. This problem with $M = 2$ phases and $N = 3$ components is solved on a block of size $600 \times 400 \times 40\,\mathrm{m}^3$ which is discretized using $24 \times 16 \times 16$ cartesian cells.

The domain is initialized with methane at a pressure of 364 bar and a saturation of $S_1 = 85\%$ except for the bottom layer where $S_1 = 0$ is used. We use an acceleration of $-9.81\,\mathrm{m/s}^2$ in vertical direction due to gravity and a constant temperature of 40 °C. The porosity is 30% all over the domain, and we have two layers with different permeability: The lower layer has a thickness of 22 m and a permeability of $K = 10^{-12}\,\mathrm{m}^2$, whereas $K = 10^{-13}\,\mathrm{m}^2$ is used for the upper one. The relations for the capillary pressure as well as the relative permeability are of Brooks–Corey type with the uniform shape parameter $\lambda = 2$ and an entry pressure of $p_e = 10^4$ Pa.

No-flow boundary conditions are applied everywhere for the first 10^{11} seconds such that a realistic steady state is reached. Afterwards, the boundary conditions are changed at the right lower front corner of the block such that carbon dioxide is injected at a rate of 10 kg/s. In addition, the steady-state values are used as Dirichlet conditions on the left back edge of the cube, representing an extraction well. The evolution of this process is illustrated in Figure 6, where the gas saturation as well as the concentrations of methane and CO_2 are shown at different time instants. The evolution of the active sets representing the phase composition is depicted in Figure 7a, whereas Figure 7b illustrates the superlinear convergence of the Newton iteration at several time steps after the start of the CO_2 injection.

Finally, Figure 8a shows the total production rates of methane, water and carbon dioxide with respect to time, whereas Figure 8b depicts the mass fraction of the components in the produced gas. We find that the break-through time of CO_2 is approximately $2.5 \cdot 10^7$ s which corrosponds to 289 days. If a CO_2 mass fraction of 50% is acceptable, methane can be produced for approximately 650 days.

5 Summary and conclusion

In this work, we have presented a new way of incorporating phase transitions into the simulation of multi-phase, multi-component processes in porous media. The conditions for the local existence of a given phase are formulated as a set of KKT conditions and rewritten in terms of a nonlinear complementarity function. Together with the discretized balance equations, these nondifferentiable but semismooth functions yield a nonlinear system which is solved iteratively by a generalized version of the Newton method. By this, there is no need for an outer iteration for the determination of the phases. In addition, some of the degrees of freedom can locally be eliminated by static condensation, such that the size of the linear system to be solved is not increased. Thus, the simulation of one time step is as efficient as one step of the approach described in [5]. However, the new scheme has an increased robustness with respect to phase transitions and the initialization of the phase distribution, such that larger time steps can be applied. This leads to a substantial gain in computational efficiency and, in some cases, only makes simulating such complex miscible multi-phase flow processes feasible.

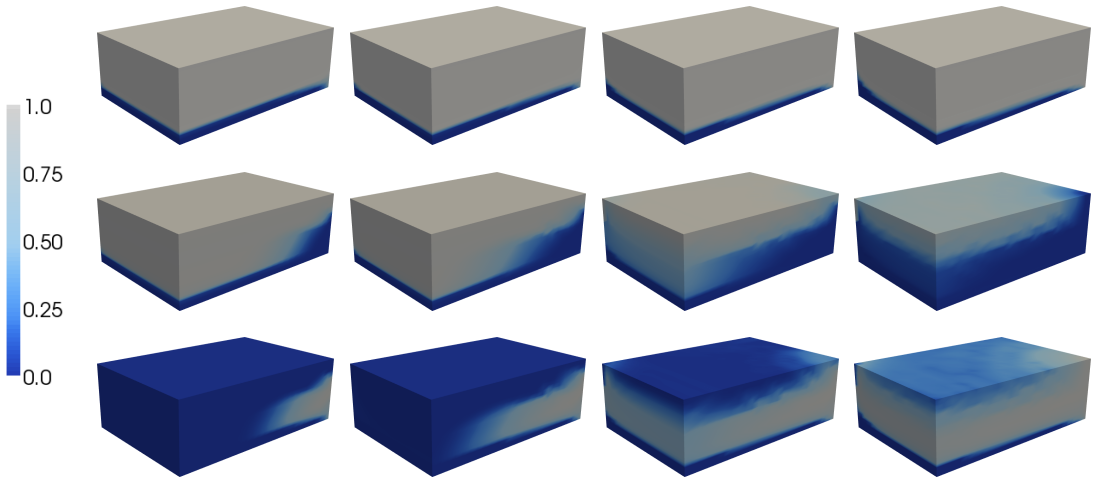

(a) $t = 7.7 \cdot 10^7$ s (b) $t = 2.3 \cdot 10^8$ s (c) $t = 7.4 \cdot 10^8$ s (d) $t = 1.8 \cdot 10^9$ s

Fig. 6: The evolution of the gas saturation (upper row) and the concentrations of methane and carbon dioxide (middle and lower row) of the sequestration problem. Time is measured after infiltration of CO_2, and the height of the block is amplified by a factor of 5.

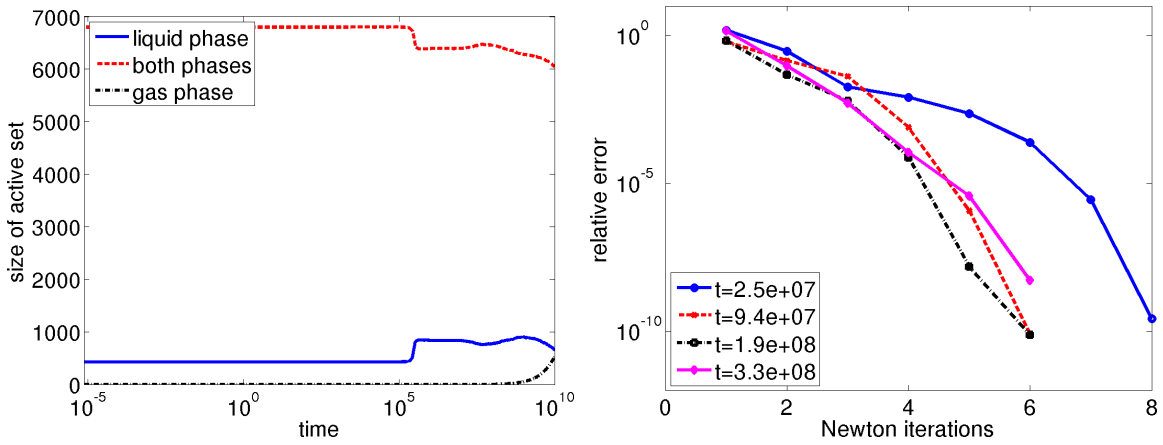

(a) Evolution of active sets (b) Convergence of Newton iteration

Fig. 7: The evolution of the size of the active sets after the start of the CO_2 injection and the relative error of the Newton iteration at different time steps.

References

1. Acosta, M.; Merten, C.; Eigenberger, G.; Class, H.; Helmig, R.; Thoben, B. & Müller-Steinhagen, H.: Modeling non-isothermal two-phase multicomponent flow in the cathode of PEM fuel cells. *J. Power Sources* **159** (2006), 1123–1141.
2. Alart, P. & Curnier, A.: A mixed formulation for frictional contact problems prone to Newton like solution methods. *Comput. Methods Appl. Mech. Engrg.* **92** (1991), 353–375.
3. Barrett, R.; Berry, M.; Chan, T. F.; Demmel, J.; Donato, J.; Dongarra, J.; Eijkhout, V.; Pozo, R.; Romine, C. & der Vorst, H. V.: *Templates for the solution of linear systems: Building blocks for iterative methods, 2nd Edition*. SIAM 1994.
4. Christensen, P. W.: A nonsmooth Newton method for elastoplastic problems. *Comput. Methods Appl. Mech. Engrg.* **191** (2002), 1189–1219.

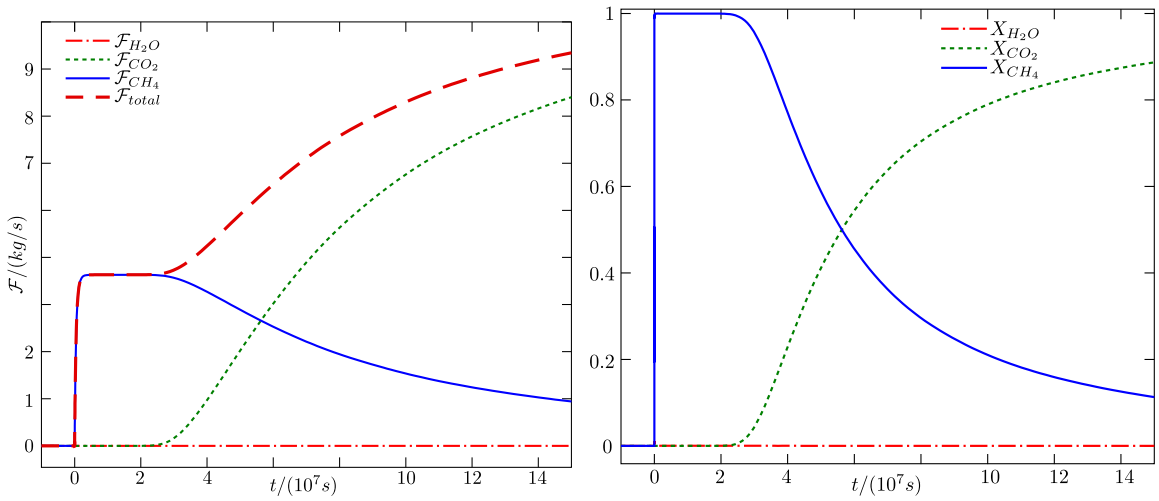

(a) Mass flows of produced gas (b) Component mass fraction of produced gas

Fig. 8: The extraction rates and the composition of the produced gas at the extraction well.

5. Class, H.; Helmig, R. & Bastian, P.: Numerical simulation of non-isothermal multiphase multicomponent processes in porous media. 1. An efficient solution technique. *Adv. Water Resour.* **25** (2002), 533–550.
6. Deuflhard, P.: *Newton methods for nonlinear problems – Affine invariance and adaptive algorithms.* Springer, Berlin Heidelberg 2004.
7. Facchinei, F. & Pang, J.-S.: *Finite-dimensional variational inequalities and complementary problems.* Springer, New York 2003.
8. Falta, R. W.; Pruess, K.; Javandel, I. & Witherspoon, P. A.: Numerical modeling of steam injection for the removal of nonaqeous phase liquids from the subsurface. 1. Numerical formulation. *Water Resour. Res.* **28** (1992), 433–449.
9. Fritz, J.; Flemisch, B. & Helmig, R.: Multiphysics modeling of advection-dominated two-phase compositional flow in porous media. *Intern. J. Numerical Analysis & Modeling* (2009), submitted, preprint on www.nupus.uni-stuttgart.de number 2009/8.
10. Geiger, C. & Kanzow, C.: *Theorie und Numerik restringierter Optimierungsaufgaben.* Springer, Berlin Heidelberg 2002.
11. Glowinski, R.; Lions, J. L. & Trémolières, R.: *Numerical analysis of variational inequalities.* North-Holland, Amsterdam 1981.
12. Hager, C. & Wohlmuth, B.: Semismooth Newton methods for variational problems with inequality constraints. *GAMM-Mitt.* **33** (2010), 8–24.
13. Helmig, R.: *Multiphase flow and transport processes in the subsurface – A contribution to the modeling of hydrosystems.* Springer Heidelberg 1997.
14. Hintermüller, M.; Ito, K. & Kunisch, K.: The primal-dual active set strategy as a semi–smooth Newton method. *SIAM J. Optim.* **13** (2003), 865–888.
15. Hüeber, S. & Wohlmuth, B.: A primal-dual active set strategy for non-linear multibody contact problems. *Comput. Methods Appl. Mech. Engrg.* **194** (2005), 3147–3166.
16. IAPWS: Release on the IAPWS industrial formulation 1997 for the thermodynamic properties of water and steam. http://www.iapws.org (1997), (Int. Assoc. for the Properties of Water and Steam).
17. IAPWS: Guideline on the Henry's constant and vapor-liquid distribution constant for gases in H2O and D2O at high temperatures. http://www.iapws.org (2004), (Int. Assoc. for the Properties of Water and Steam).
18. IAPWS: Release on the IAPWS formulation 2008 for the viscosity of ordinary water substance. http://www.iapws.org (2008).

19. IPCC: *Special Report on Carbon Dioxide Capture and Storage*. Tech. rep., (Intergovernmental Panel on Climate Change) (2005).
20. Ito, K. & Kunisch, K.: Semi-smooth Newton methods for variational inequalities of the first kind. *M2AN, Math. Model. Numer. Anal.* **37** (2003), 41–62.
21. Ito, K. & Kunisch, K.: The primal-dual active set method for nonlinear optimal control problems with bilateral constraints. *SIAM J. Control. Optim.* **43** (2004), 357–376.
22. Kikuchi, N. & Oden, J.: *Contact problems in elasticity: A study of variational inequalities and finite element methods*. SIAM Studies in Applied Mathematics, Philadelphia 1988.
23. Kinderlehrer, D. & Stampacchia, G.: *An introduction to variational inequalities and their applications*. SIAM 2000.
24. Kunisch, K. & Rösch, A.: Primal-dual active set strategy for a general class of constrained optimal control problems. *SIAM J. Optim.* **13** (2002), 321–334.
25. Leverett, M.: Capillary behavior in porous solids. *AIME Petroleum Transactions* **142** (1941), 152–169.
26. Mifflin, R.: Semismooth and semiconvex functions in constrained optimization. *SIAM J. Control Optim.* **15** (1977), 959–972.
27. Niessner, J. & Helmig, R.: Multi-scale modeling of three-phase-three-component processes in heterogeneous porous media. *Adv. Water Resour.* **30** (2007), 2309–2325.
28. Popp, A.; Gee, M. W. & Wall, W. A.: A finite deformation mortar contact formulation using a primal–dual active set strategy. *Internat. J. Numer. Methods Engrg.* **79** (2009), 1354–1391.
29. Qi, L. & Sun, J.: A nonsmooth version of Newton's method. *Math. Prog.* **58** (1993), 353–367.
30. Saad, Y.: *Iterative methods for sparse linear systems*. SIAM, Philadelphia 2003, 2 edn.
31. Starr, R. C. & Cherry, J. A.: In situ remediation of contaminated ground water: the funnel-and-gate system. *Ground Water* **32** (1994), 465–476.
32. Udell, K. S.: Heat transfer in porous media considering phase change and capillarity – the heat pipe effect. *Intern. J. Heat Mass Transfer* **28** (1985), 485–495.